THE JOURNAL OF BIOLOGICAL CHEMISTRY VOL. 283, NO. 39, pp. 26782–26794, September 26, 2008
© 2008 by The American Society for Biochemistry and Molecular Biology, Inc. Printed in the U.S.A.

Oligomeric Structure and Minimal Functional Unit of the Electrogenic Sodium Bicarbonate Cotransporter NBCe1-A*

Received for publication, May 26, 2008, and in revised form, July 22, 2008 Published, JBC Papers in Press, July 25, 2008, DOI 10.1074/jbc.M804006200

Liyo Kao[‡], Pakan Sassani[‡], Rustam Azimov[‡], Alexander Pushkin[‡], Natalia Abuladze[‡], Janos Peti-Peterdi[§], Weixin Liu[‡], Debra Newman[‡], and Ira Kurtz[‡1]

From the [‡]Division of Nephrology, David Geffen School Medicine, UCLA, Los Angeles, California 90095-1689 and the [§]Departments of Physiology and Biophysics and Medicine, Zilkha Neurogenetic Institute, Keck School of Medicine, University of Southern California, Los Angeles, California 90033

The electrogenic sodium bicarbonate cotransporter NBCe1-A mediates the basolateral absorption of sodium and bicarbonate in the proximal tubule. In this study the oligomeric state and minimal functional unit of NBCe1-A were investigated. Wild-type (wt) NBCe1-A isolated from mouse kidney or heterologously expressed in HEK293 cells was predominantly in a dimeric state as was shown using fluorescence energy transfer, pulldown, immunoprecipitation, cross-linking experiments, and nondenaturing perfluorooctanoate-PAGE. NBCe1-A monomers were found to be covalently linked by S–S bonds. When each of the 15 native cysteine residues were individually removed on a wt-NBCe1-A backbone, dimerization of the cotransporter was not affected. In experiments involving multiple native cysteine residue removal, both Cys^{630} and Cys^{642} in extracellular loop 3 were shown to mediate S–S bond formation between NBCe1-A monomers. When native NBCe1-A cysteine residues were individually reintroduced into a cysteineless NBCe1-A mutant backbone, the finding that a Cys^{992} construct that lacked S–S bonds functioned normally indicated that stable covalent linkage of NBCe1-A monomers was not a necessary requirement for functional activity of the cotransporter. Studies using concatameric constructs of wt-NBCe1-A, whose activity is resistant to methanesulfonate reagents, and an NBCe1-A^{T442C} mutant, whose activity is completely inhibited by methanesulfonate reagents, confirmed that NBCe1-A monomers are functional. Our results demonstrate that wt-NBCe1-A is predominantly a homodimer, dependent on S–S bond formation that is composed of functionally active monomers.

Bicarbonate absorption by the proximal tubule of the kidney plays an important role in the regulation of the plasma bicarbonate concentration and in systemic acid-base balance. Decreased proximal tubule bicarbonate absorption causes proximal renal tubular acidosis (1–4). Familial autosomal recessive proximal renal tubular acidosis results from mutations in the electrogenic sodium bicarbonate cotransporter NBCe1-A encoded by the *SLC4A4* gene (5, 6). Mice lacking NBCe1 also have severe proximal renal tubular acidosis (7). These findings confirm that flux through the cotransporter is the predominant process mediating bicarbonate absorption across the basolateral membrane of the proximal tubule (8).

In addition to NBCe1, other SLC4 proteins are known to be associated with various diseases/phenotypes. Specifically, abnormalities in the function of the anion exchanger AE1 (*SLC4A1* gene) cause distal renal tubular acidosis and red blood cell abnormalities (9–12). Polymorphisms in the anion exchanger AE3 (*SLC4A3*) and transgenic mice studies indicate a role in preventing seizures (13, 14). Mice with loss of NBCn1 (SLC4A7) exhibit combined blindness and abnormal hearing and are a model for Usher syndrome 2B in humans (15). Polymorphisms in the electrogenic sodium bicarbonate cotransporter NBCe2 (*SLC4A5*) are associated with hypertension (16). Finally, mutations in NaBC1, the electrogenic sodium borate cotransporter encoded by *SLC4A11*, cause CHED2 disease, Harboyan syndrome, and Fuchs endothelial corneal dystrophy (17–20).

NBCe1-A is composed of 1035 amino acids and has a predicted minimum molecular mass of 116 kDa (6). The estimated molecular mass of glycosylated NBCe1-A is ~130–145 kDa (21). According to NBCe1-A topology models based on hydropathy analysis, the cotransporter is predicted to have between 10 and 14 transmembrane segments (22). Tatishchev *et al.* (22) have shown that that the cotransporter spans the membrane a minimum 10 times with the N and C termini of NBCe1-A localized intracellularly. Based on AE1 topology (23) the cotransporter may have up to 13 transmembrane regions with two re-entrant loops (24). Studies of the oligomeric structure of AE1 have shown that it forms dimers and tetramers under nondenaturing conditions (25–27), and tetramers of AE3 have been isolated from rabbit kidney membranes (28). Preliminary studies showed that NBCe1-A forms oligomers (29) and that the cytoplasmic N terminus of NBCe1-A is dimeric (30).

Given its importance in proximal tubule bicarbonate absorption, systemic acid-base balance, and in human disease, in this study we characterized the oligomeric structure of NBCe1-A and determined the minimal functional unit of the cotransporter. The following questions were addressed in our experiments. 1) Is NBCe1-A an oligomer? 2) What is the oligomeric state of NBCe1-A? 3) What is the role of S–S bonds in the

* This work was supported, in whole or in part, by National Institutes of Health Grants DK077162, DK058563, DK063125, ES12935, DK64324, and DK74754. The costs of publication of this article were defrayed in part by the payment of page charges. This article must therefore be hereby marked "*advertisement*" in accordance with 18 U.S.C. Section 1734 solely to indicate this fact.

[1] To whom correspondence should be addressed: UCLA Division of Nephrology, 10833 Le Conte Ave., Rm. 7-155 Factor Bldg., Los Angeles, CA 90095-1689. E-mail: ikurtz@mednet.ucla.edu.

Downloaded from www.jbc.org by guest, on September 29, 2009

oligomerization of NBCe1-A? 4) What is the minimal functional unit of NBCe1-A?

EXPERIMENTAL PROCEDURES

Membrane Isolation from Mouse Kidney—All animal procedures were approved by the Institutional Animal Care and Use Committee of UCLA. All procedures were performed at 4 °C. Mouse kidney (~0.5 g) was disrupted in a glass homogenizer in 600 μl of cell lysis solution (200 mM Tris-HCl, pH 7.5), containing 1 μg/ml pepstatin and 1 tablet of Complete protease inhibitor mixture (Roche Applied Science) per 2 ml of solution. The tissue homogenate was homogenized initially and then passed 40 times through a 25-gauge needle (BD Biosciences). Tissue homogenates were centrifuged at 600 × *g* for 10 min and then at 18,000 × *g* for 10 min. The resulting supernatant was centrifuged at 200,000 × *g* for 1 h. The precipitate of mouse kidney membranes was used for analysis.

Transfection of Cells and Cell Culture—HEK293 cells (American Type Culture Collection) were grown at 37 °C, 5% CO_2, in Dulbecco's modified Eagle's medium (DMEM)[2] supplemented with 10% fetal bovine serum, 200 mg/liter L-glutamine, and penicillin/streptomycin mixture (Gemini Bio-Products, West Sacramento, CA). For immunoblot expression experiments, HEK293 cells growing on 10-cm plates at 80–90% confluency were transiently transfected using Lipofectamine 2000 (Invitrogen) according to the manufacturer's protocol. 2 h later the transfection medium was replaced with fresh DMEM containing 10% fetal bovine serum. Plates were incubated at 37 °C (5% CO_2) for 24 h prior to use for immunoblot analysis. For immunohistochemistry and experiments involving the study of NBCe1-A transport, the cells were split onto glass coverslips coated with fibronectin in a 6-well plate and transfected the following day at 80–90% confluency with Lipofectamine 2000. Immunohistochemical and functional studies were performed 24 h later.

Membrane Isolation from Cultured Cells—HEK293 cells were collected from 10-cm cultured plate, washed three times with ice-cold phosphate-buffered saline (PBS, Invitrogen), and suspended at 4 °C in 250 μl of 200 mM Tris-HCl, pH 7.5, containing 1 μg/ml pepstatin and Complete protease inhibitor mixture (1 tablet/2 ml). Cells were then homogenized by passing 10 times through a 25-gauge needle, centrifuged at 600 × *g* for 10 min, then at 18,000 × *g* for 10 min, and finally at 200,000 × *g* for 1 h. The resulting pellet was used for analysis. In some studies, the total cell lysate was analyzed where indicated.

SDS-PAGE—50 μl of membrane pellet was mixed with an equal volume of 2× SDS sample buffer containing 0.125 M Tris-HCl, pH 6.8, 20% glycerol, 4% SDS, with or without 0.2 M dithiothreitol (DTT; final concentration 0.1 M), and 0.005% bromphenol blue and incubated at 95 °C for 5 min. Proteins were separated on 4–8 or 7.5% polyacrylamide gels (Jule, Milford, CT) at 100 V.

Nondenaturing PFO-PAGE—All experiments were performed using either 7.5 or 4–8% gradient precast Tris-glycine mini gels (Jule, Milford, CT). Running Tris-glycine buffer contained PFO (Oakwood Products, West Columbia, SC). PFO-PAGE was performed as described previously (31). Briefly, 50 μl of crude membranes was mixed with an equal volume of sample buffer containing 125 mM Tris, 8% PFO, 20% glycerol, with or without 0.2 M DTT, and 0.005% bromphenol blue, pH 8.0. The sample was vortexed and incubated at room temperature for 30 min. Proteins were resolved by PFO-PAGE at 100 V.

Immunoblotting—Following PFO- or SDS-PAGE, the proteins were electrotransferred onto Hybond-P polyvinylidene difluoride membranes (GE Healthcare) as described (22). Nonspecific binding was blocked by incubation for 1 h in Tris-buffered saline (TBS: 20 mM Tris-HCl, pH 7.5, 140 mM NaCl) that contained 5% dry milk and 0.05% Tween 20 (Bio-Rad). The following primary antibodies were used: rabbit anti-human N-terminal NBCe1-A-specific (32) and C-terminal NBC1-specific (NBC1-4B2), (22) antibodies at 1:1,000 dilution, mouse anti-His_6 antibody (Invitrogen), and rabbit anti-GFP (Invitrogen) antibodies at a dilution of 1:5,000. Secondary horseradish peroxidase-conjugated species-specific antibodies from Jackson ImmunoResearch (West Grove, PA) were used at 1:10,000 dilution. Primary and secondary antibodies were incubated with the membranes for 1 h at room temperature. The bands were visualized using an ECL kit and Hyperfilm ECL (GE Healthcare). The apparent molecular masses were determined by log-linear curve fitting of the molecular weight standards indicated for each gel. Immunoblotting was performed four times for each experimental protocol.

Pulldown and Coimmunoprecipitation Experiments—NBCe1-A was subcloned into pEGFP-C3 (BD Biosciences) using the EcoRI and ApaI sites to create an N-terminal EGFP tag (EGFP-NBCe1-A). NBCe1-A containing an N-terminal His_6 tag (His_6-NBCe1-A) was also generated in the pcDNA3.1 vector. Both constructs were expressed individually or together in HEK293 cells. Crude membranes were isolated from the cells as described above and mixed with equal volume of 200 mM Tris-HCl, pH 7.5, containing 1 μg/ml pepstatin and Complete protease inhibitor mixture (1 tablet/2 ml) and 1% *n*-dodecyl-β-D-maltoside. Samples were then incubated at 4 °C for 30 min with gentle agitation, mixed with either Ni^{2+}-NTA Superflow agarose beads (Qiagen) or the anti-GFP antibody (Invitrogen) pre-coupled to protein A-Sepharose (GE Healthcare), and incubated at 4 °C while rotating overnight. Proteins bound to Ni^{2+}-NTA Superflow agarose beads were eluted with 300 mM imidazole in binding buffer. The samples were mixed with an equal volume of 2× SDS sample buffer containing DTT (DTT final concentration 0.1 M) and analyzed by SDS-PAGE. Agarose beads alone were used as a negative control in the Ni^{2+}-NTA Superflow agarose beads experiments. Proteins bound to protein A-Sepharose beads were eluted with 0.1 M glycine, pH 3, and the samples were neutralized by adding 1 M Tris-HCl, pH 9, mixed with sample buffer as described, and analyzed by SDS-PAGE. Nonspecific IgG was used as a negative control.

[2] The abbreviations used are: DMEM, Dulbecco's modified Eagle's medium; FRET, fluorescence energy transfer; wt, wild type; EYFP, enhanced yellow fluorescent protein; GFP, green fluorescent protein; EGFP, enhanced GFP; DTT, dithiothreitol; PFO, perfluorooctanoate; MTS, methanethiosulfonate; MTSES, sodium (2-sulfonatoethyl)methanethiosulfonate; NTA, nitrilotriacetic acid; PBS, phosphate-buffered saline; BCECF, 2′,7′-bis(carboxyethyl)-5,6-carboxyfluorescein.

Downloaded from www.jbc.org by guest, on September 29, 2009

Immunocytochemistry—The coverslips were rinsed twice with 1× PBS and then incubated with 1 ml of cold methanol for 2 min. Methanol was then removed by rinsing with 1× PBS. The well characterized NBCe1-A-specific N-terminal antibody (32) was applied at 1:100 dilution in PBS for 1 h at room temperature. After several washes in PBS, goat anti-rabbit IgG conjugated with Cy3 (1:500 dilution; Jackson ImmunoResearch) was applied for 1 h at room temperature. The slides were rinsed in PBS and mounted in Crystal/Mount (Biomeda, Foster City, CA). A PXL charge-coupled device camera (model CH1; Photometrics), coupled to a Nikon Microphot-FXA epifluorescence microscope, was used to capture and digitize the fluorescence images for image acquisition.

Molecular Mass of NBCe1-A—Protein standards and purified NBCe1-A were mixed with PFO sample buffer to a final concentration of 1% PFO, and loaded onto 7.5% Tris-Gly gel (Jule, Milford, CT). PFO-PAGE was performed as described before, and the proteins were analyzed by either silver staining or immunoblotting. The protein standards (Sigma) used were as follows: 1) urease (monomer, 91 kDa; dimer, 182 kDa; trimer, 273 kDa); 2) albumin (monomer, 66 kDa; dimer, 132 kDa; trimer, 198 kDa; tetramer, 264 kDa); 3) apoferritin (443 kDa); 4) alcohol dehydrogenase (150 kDa); and 5) β-amylase (200 kDa). 50 ng of each protein standard was loaded onto the gel, and a silver stain was done (Silver Stain Plus kit, Bio-Rad).

Purification of AE1 Protein—The accuracy of the protein standard calibration curve discussed in the previous protocol was confirmed using AE1 protein because it is a well characterized membrane protein and shares sequence homology with NBCe1-A. Bovine red blood cell membrane ghosts were prepared from fresh bovine blood as described previously (33). The red blood cell ghosts (5 ml) were then extracted with 50 mM Tris-HCl, pH 7.5, containing 1% C12E8 (Anatrace, Maumee, OH) and 1 mM phenylmethylsulfonyl fluoride for 1 h at 4 °C, and insoluble membranes were precipitated by ultracentrifugation at 150,000 × *g* for 45 min. The supernatant was then loaded on a 2 × 8-cm column of diethylaminoethylcellulose (DE-52, Whatman) pre-equilibrated with the 50 mM Tris-HCl, pH 7.5. The column was washed with the same buffer and then with 50 mM Tris-HCl, pH 7.5, containing 100 mM NaCl. The fraction eluted with 50 mM Tris-HCl, pH 7.5, containing 200 mM NaCl, was loaded onto 1 × 5-cm hydroxyapatite (Sigma) column equilibrated with 10 mM sodium phosphate, pH 8.0. AE1 was eluted with 100 mM sodium phosphate and concentrated using Microcon YM-100 filter units (Millipore, Temecula, CA).

NBCe1-A Cross-linking—To covalently cross-link membrane-embedded NBCe1-A proteins extracellularly, a water-soluble homobifunctional *N*-hydroxysuccinimide ester BS^3 (Pierce) was used. BS^3 is a water-soluble homobifunctional *N*-hydroxysuccinimide ester with an arm length of 11.4 Å that reacts with primary amino groups. BS^3 is not membrane-permeable and is used to form covalent bonds only between external parts of membrane-embedded proteins. NBCe1-A was transiently expressed in HEK293 cells. 24 h after transfection, the cells were harvested from a 10-cm cultured plate, suspended, and washed three times in ice-cold PBS. BS^3 was added to a final concentration of 5 mM, and the cell suspension was incubated at room temperature for 30 min. Control samples were incubated with PBS alone. The reaction was stopped by adding 1 M Tris-HCl, pH 8.0, to a final concentration 100 mM, and incubation was at room temperature for 15 min. The cells were then centrifuged at 600 × *g* for 2 min and washed twice with ice-cold PBS. The pellet was resuspended in 250 ml of lysis solution (200 mM Tris-HCl, pH 7.5, 1 mg/ml pepstatin, and 1 tablet of Complete Mini protease inhibitor mixture per 2 ml (Roche Applied Science)). The cells were then lysed; the membranes were isolated, and membrane proteins were analyzed by SDS-PAGE and immunoblotting as described above.

Fluorescence Resonance Energy Transfer (FRET)—HEK293 cells (American Type Culture Collection) were grown at 37 °C, 5% CO_2, in DMEM supplemented with 10% fetal bovine serum, 200 mg/liter L-glutamine, and penicillin/streptomycin mixture (Gemini Bio-Products). 24 h before transfection, a fully confluent 10-cm polystyrene plate (BD Biosciences) of cells was split 1:3 onto a plate with 12 ml of medium that was then immediately divided into a 6-well plate (2 ml/well) containing coated coverslips. 24 h later, the 80% confluent coverslips were transfected with NBCe1 constructs. Two NBCe1 constructs were used in these studies. The first construct consisted of NBCe1-A tagged on its N terminus with Cerulean fluorescent protein (34) (Cer-NBCe1-A). NBCe1-A was subcloned into the Cerulean vector between BglII and ApaI sites. In the second construct, NBCe1-A was tagged on its N terminus with EYFP (EYFP-NBCe1-A) between EcoRI-ApaI site in the pEYFP-C1 vector (BD Biosciences). The plasmids containing these constructs were transfected into HEK293 cells grown in coated coverslips in 6-well plates using Lipofectamine 2000 (Invitrogen). The transfection medium was removed after 2 h and replaced with fresh DMEM with 10% fetal bovine serum without antibiotics until the following day when the FRET experiments were performed.

FRET between Cerulean-NBCe1-A and EYFP-NBCe1-A was assessed by calculating the sensitized emission (the EYFP emission upon Cerulean excitation) from confocal donor and acceptor images, acquired separately using a multiphoton fluorescence microscope. The imaging equipment consisted of a Leica TCS SP2 confocal microscope system (Leica Microsystems, Heidelberg, Germany), a DM IRE2 inverted microscope powered by a wide band, fully automated, infrared (710–920 nm) combined photo-diode pump laser and mode-locked titanium: sapphire laser (Mai-Tai, Spectra-Physics, Mountain View, CA), and a blue argon 514 nm/20-milliwatt laser.

Cerulean fluorescence protein was excited using optimized donor excitation with the multiphoton laser at 820 nm (34). Spectral detection bandwidth of the Leica SP2 channels was set up to balance minimal cross-talk with optimal collection efficiency (35). Cerulean fluorescence protein emission was detected between 460 and 490 nm; EYFP was excited with a 514 nm argon laser, and emission was detected between 528 and 603 nm. FRET between Cerulean fluorescent protein and EYFP was calculated using the FRET sensitized emission module of the Leica confocal software (LCS 2.61.1537) applying the equation: $FRET = B - b \cdot A - (c - a \cdot b) \cdot C$, where A = Cerulean emission (by Cerulean excitation); B = FRET emission (by Cerulean excitation); C = EYFP emission (by EYFP excitation); a = correction factor of EYFP only measurement (A/C when only EYFP is expressed); b = correction factor of Cerulean only

Downloaded from www.jbc.org by guest, on September 29, 2009

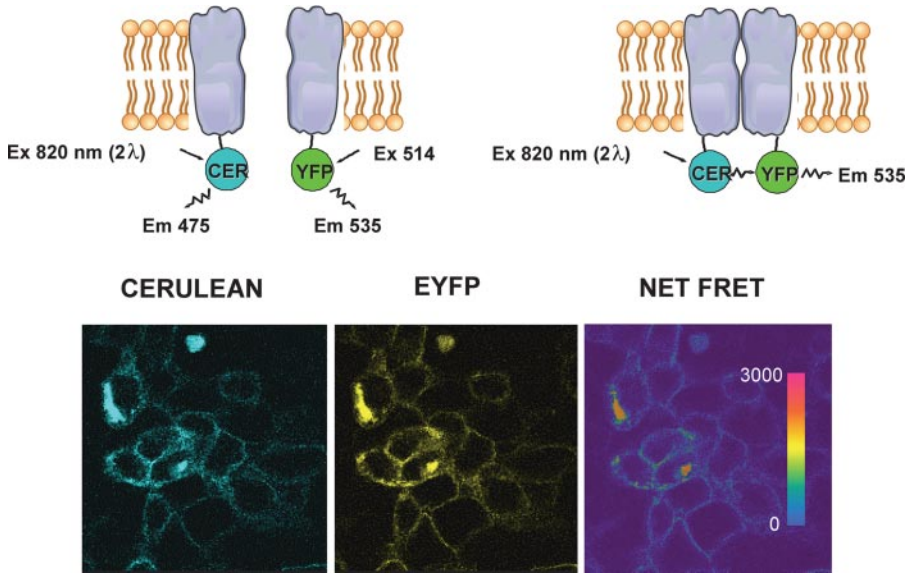

FIGURE 1. **Sensitized FRET emission between Cerulean-NBCe1-A and EYFP-NBCe1-A at the cell membrane.** *Top panel* is a schematic of the FRET experiments showing the two-photon (2λ) excitation (*Ex 820 nm*) of Cerulean (*CER*) or visible excitation of EYFP (*Ex 514 nm*) and their respective emissions. In contrast to the absence of interaction between NBCe1-A-linked Cerulean and EYFP (*left upper panel*), NBCe1-A dimerization results in FRET between Cerulean and EYFP (*right upper panel*). Cerulean and EYFP images (*lower panel*) of HEK293 cells expressing Cerulean-NBCe1-A and EYFP-NBCe1-A were acquired on a confocal microscope and total donor (*Cerulean*), total acceptor (*EYFP*), and sensitized FRET emission (*NET FRET*) were calculated as described under "Experimental Procedures." Both Cerulean, EYFP, and NET FRET signals were found mainly in the cell membrane, whereas no significant FRET was observed intracellularly. Cerulean and EYFP images were 12-bit resolution (scaled from 0 to 4096); the FRET signal was scaled from 0 to 3000 and intensity colored as shown.

measurement (EYFP emission by Cerulean excitation/*A* when only Cerulean is expressed), and *c* = correction factor of EYFP only measurement (EYFP emission by Cerulean excitation/*C* when only EYFP is expressed). Factors *a, b,* and *c* in the acquired images were 0.038, 0.427, and 0.055, respectively.

Construction of NBCe1-A Cysteine Mutants—Mutations in the full-length human NBCe1-A were performed using a QuickChange site-directed mutagenesis kit (Invitrogen). For certain protocols, a cysteineless mutant was created by replacing all 15 native cysteines with serine residues. The cysteineless mutant was used as a backbone for generating additional constructs where in each of the positions, where cysteine residues were normally located, a native cysteine residue was replaced individually in separate constructs one at a time. A total of 15 additional constructs was generated in this fashion. In other experiments, the wt-NBCe1-A backbone was used to generate cysteine mutants in which individual native cysteine residues were removed one at a time leaving the remaining native cysteines in place. In total, 15 separate mutants were generated. Finally, additional mutants were generated where multiple cysteine residues were removed on the wt-NBCe1-A backbone from extracellular loop 3.

Construction of NBCe1-A Concatamers—In experiments involving the use of concatameric constructs, we took advantage of our recent finding that the NBCe1-A^{T442C} mutant functions normally but can be completely inhibited by MTS reagents (36). In contrast, these agents have no effect of wt-NBCe1-A. The following concatameric constructs of wt-NBCe1-A and NBCe1-A^{T442C} were studied: wt-NBCe1-A-linker-wt-NBCe1-A; wt-NBCe1-A-linker-NBCe1-A^{T442C}; NBCe1-A^{T442C}-linker-wt-NBCe1-A; and NBCe1-A^{T442C}-linker-NBCe1-A^{T442C}. The two individual units were linked through a linker peptide (Thr-Gly) in pcDNA3.1/neo vector (Invitrogen). To insert the linker peptide, the first unit (either wt-NBCe1-A or the T442C mutant) was cloned in pcDNA 3.1 vector (Invitrogen) between EcoRI and XhoI sites. An AgeI (Thr-Gly) site was introduced at the 3′ end of the first unit by site-directed mutagenesis (Stratagene) instead of the stop codon. The second unit (either the T442C mutant or wt-NBCe1-A) was made using the PCR and inserted between AgeI and XhoI sites in the first construct. Immunoblot analysis of the concatameric constructs was performed as described above. Flux through the four concatamers was measured using BCECF-AM as discussed below. MTSES was stored under argon at −20 °C and dissolved in water to a final concentration immediately before each experiment. The cells were exposed to MTSES (4 mM) for 5 min after the loading period with BCECF-AM was completed in the absence of Na^+. Sequences of all constructs were confirmed by bi-directional sequencing using an ABI 310 sequencer (PerkinElmer Life Sciences).

Na^+-dependent Base Flux Mediated by NBCe1-A, NBCe1-A Mutants, and NBCe1-A Concatamers—HEK293 cells were grown on fibronectin-coated coverslips and were transiently transfected with various constructs using Lipofectamine 2000 (Invitrogen). Mock-transfected cells were transfected with the vector alone. The plasmids were purified with the Endofree plasmid purification kit (Qiagen) prior to their use. Functional studies were performed 24 h post-transfection. Intracellular pH was monitored using the fluorescent probe BCECF (Molecular Probes, Eugene, OR) and a microfluorometer coupled to the microscope (37). Data were obtained from ~20 cells per coverslip. A minimum of five different coverslips was studied for each construct. Calibration of intracellular BCECF was performed at the end of every experiment by monitoring the 500/440-nm fluorescence excitation ratio at various values of intracellular pH (pH_i) in the presence of high K^+ nigericin standards. The cells were initially bathed for 25 min in a Na^+-free, Cl^--containing HEPES-buffered solution containing (in mM) the following : tetramethylammonium chloride 140, K_2HPO_4 2.5, $CaCl_2$ 1, $MgCl_2$ 1, and glucose 5; pH 7.4. The cells were acutely acidified to pH ~6.7 by exposure to HCO_3^--buffered Na^+-free, Cl^--containing solution containing (in mM) the following: tetramethylammonium chloride 115, K_2HPO_4 2.5, $CaCl_2$ 1, $MgCl_2$ 1, glucose 5, and tetramethylammonium chloride-HCO_3 25; pH 7.4. The cells were then exposed to an HCO_3^--buffered Na^+- and Cl^--containing solution containing (in mM) the following: NaCl 115, K_2HPO_4 2.5, $CaCl_2$ 1, $MgCl_2$ 1,

Downloaded from www.jbc.org by guest, on September 29, 2009

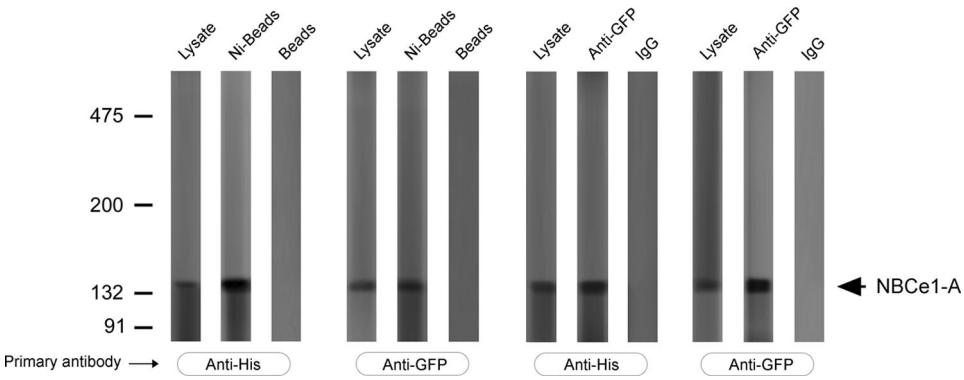

FIGURE 2. **Pulldown and immunoprecipitation studies.** His_6-NBCe1-A and EGFP-NBCe1-A constructs were coexpressed in HEK293 cells. The cells were lysed as described under "Experimental Procedures." Ni^{2+} beads were used to pull down the His_6-tagged cotransporter. Proteins bound to Ni^{2+}-NTA Superflow agarose beads were eluted with 300 mM imidazole in binding buffer. The His_6-NBCe1-A construct was detected with an anti-His_6 antibody, and EGFP-NBCe1-A was detected with an anti-GFP antibody using SDS-PAGE. The cell lysate was assayed using both antibodies. Agarose beads alone were used as a negative control in the Ni^{2+}-NTA Superflow agarose beads experiments. The converse experiment was performed wherein an anti-GFP antibody was used to immunoprecipitate the EGFP-NBCe1-A construct, and the anti-His_6 and anti-GFP antibodies were used to detect both constructs in the immunoprecipitate using SDS-PAGE. The cell lysate was assayed using both antibodies. Nonspecific IgG was used as a negative control.

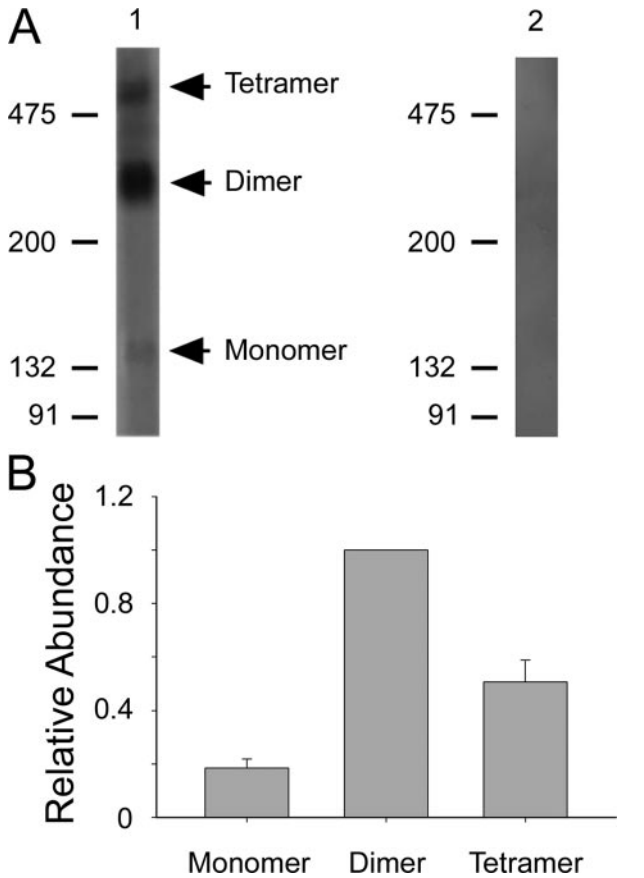

FIGURE 3. **Determination of the oligomeric structure of NBCe1-A in mouse kidney using nondenaturing conditions.** *A,* mouse renal cortex membrane fractions were run on PFO-PAGE in the absence of DTT, and immunoblots were probed with the following: *lane 1,* anti-NBCe1-A antibody; *lane 2,* immunizing peptide-blocked NBCe1-A. *B,* relative abundance of monomeric and oligomeric forms of NBCe1-A. Immunoblots were scanned, and the bands were compared using the Adobe Photoshop 9 software (Adobe Systems, San Jose, CA). The dimeric variant was assigned an arbitrary value of 1. Note that the band referred to as a tetramer could represent a dimer of NBCe1-A dimers or an NBCe1-A hetero-complex.

glucose 5, and $NaHCO_3$ 25; pH 7.4; and the initial rate (initial 15 s) of pH_i recovery was calculated. All solutions contained 5′-(*N*-ethyl-*N*-isopropyl)amiloride (5 μM) to block endogenous Na^+-H^+ exchange. Intrinsic cell buffer capacity (β_i) was measured as we described previously (38). In HCO_3^--containing solutions, the total cell buffer capacity (β_T) was equal to β_i plus the HCO_3^- buffer capacity calculated as $2.3\times [HCO_3^-\text{rsqb}]_i$. Equivalent base flux through the cotransporter was calculated as $dpH_i/dt \times (\beta_T$, where dpH_i/dt represents the initial rate of change of pH_i after exposure to the Na^+-containing solution.

RESULTS

FRET between Cerulean-NBCe1-A and EYFP-NBCe1-A—As an initial approach to investigate whether NBCe1-A monomers interact directly in living cells, we measured FRET between NBCe1-A monomers labeled in their N termini with Cerulean fluorescence protein and extended yellow fluorescence protein (EYFP) coexpressed in HEK293 cells. Both constructs were expressed on the plasma membrane of the cells, and a FRET signal was detected in the cells coexpressing both constructs (Fig. 1). The positive FRET results indicated that the distance between the two fluorophores is <10 nm and suggested that NBCe1-A monomers interact to form oligomers on the plasma membrane of HEK293 cells.

Pulldown and Immunoprecipitation Studies—To determine whether the results of the FRET experiments suggesting that NBCe1-A monomers interact *in vivo* could be confirmed, as a separate approach, pulldown and immunoprecipitation studies were done. For this purpose, two tagged NBCe1-A constructs, *e.g.* EGFP-NBCe1-A and His_6-NBCe1-A, were coexpressed in HEK293 cells. In the first series of experiments, we used Ni^{2+} beads to pull down the His_6-NBCe1-A construct and determined whether the EGFP-NBCe1-A could be pulled down simultaneously. As shown in Fig. 2, both constructs were expressed, and the cell lysate contained the His_6-NBCe1-A construct as detected using an anti-His_6 antibody, and EGFP-NBCe1-A was detected with an anti-GFP antibody. In pulldown experiments using Ni^{2+}-NTA Superflow agarose beads, both the His_6-NBCe1-A construct as well as EGFP-NBCe1-A were detected. These findings suggest that the two tagged constructs interact in HEK293 cells. In separate experiments, we used an anti-GFP antibody to immunoprecipitate the EGFP-NBCe1-A construct. As shown in Fig. 2, the immunoprecipitate contained both the EGFP- and His_6-tagged constructs. Therefore, the results of the pulldown and coimmunoprecipitation experiments complement the data obtained in the FRET studies and indicate that NBCe1-A monomers interact to form oligomers *in vivo*.

Downloaded from www.jbc.org by guest, on September 29, 2009

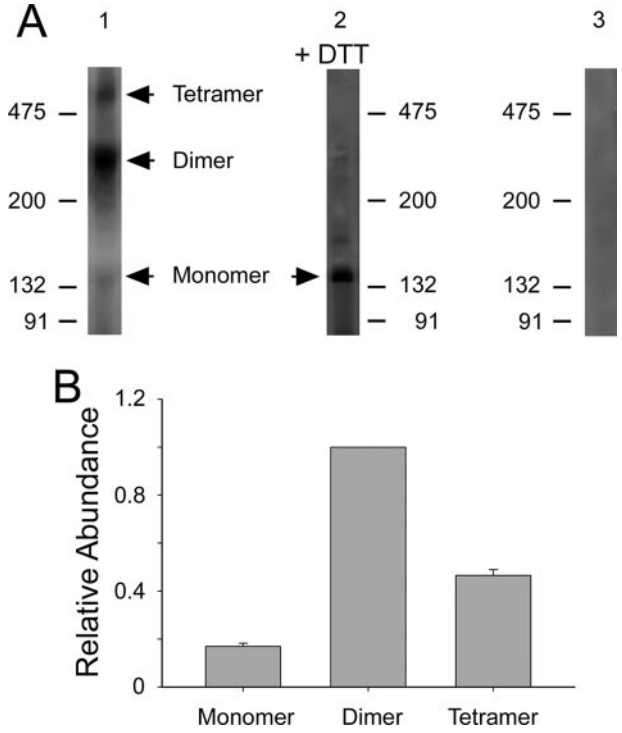

FIGURE 4. **Determination of the oligomeric structure of NBCe1-A expressed in HEK293 cells using nondenaturing conditions.** *A,* samples were subjected to PFO-PAGE as follows: *lane 1*, without DTT; *lane 2*, plus DTT; *lane 3*, mock-transfected cells and immunoblots were probed with an anti-NBCe1-A antibody. *B,* relative abundance of monomeric and oligomeric forms of NBCe1-A. Immunoblots were scanned, and the bands were compared using the Adobe Photoshop 9 software. The dimeric variant was assigned an arbitrary value of 1.

NBCe1-A Oligomerization in Mouse Kidney—Previous experiments done in cells heterologously expressing NBCe1-A have reported that the apparent monomer molecular mass of NBCe1-A is ~130–145 kDa. To determine whether native NBCe1-A is an oligomer as suggested by the results in HEK293 cells, the cotransporter was isolated from mouse kidney using the nondenaturing detergent PFO (39) in the absence of DTT and analyzed by PFO-PAGE. As shown in Fig. 3*A*, unlike previous studies in the literature that utilized denaturing conditions, a major band was detected that corresponded with the expected dimeric size and a less intense band of higher molecular weight was detected that likely represents a tetramer. Only a weak band corresponding to the monomeric form of the cotransporter was detected. The relative amount of dimeric *versus* tetrameric and monomeric forms of the cotransporter is shown in Fig. 3*B*. These results indicate that NBCe1-A is expressed in the kidney as an oligomer and that the cotransporter is predominantly a dimer.

NBCe1-A Oligomerization in HEK293 Cells—The experiments in mouse kidney using nondenaturing conditions suggested that NBCe1-A forms oligomers that consist predominantly of dimers. Further studies were done in HEK293 cells as a model system to investigate the mechanism of stable oligomerization of the cotransporter. In the presence of the nondenaturing detergent PFO in the absence of DTT as shown in Fig. 4*A*, a major band was detected at ~290 kDa that likely represents a dimer, and a less intense band of higher molecular weight was detected that could represent a tetramer, a dimer of

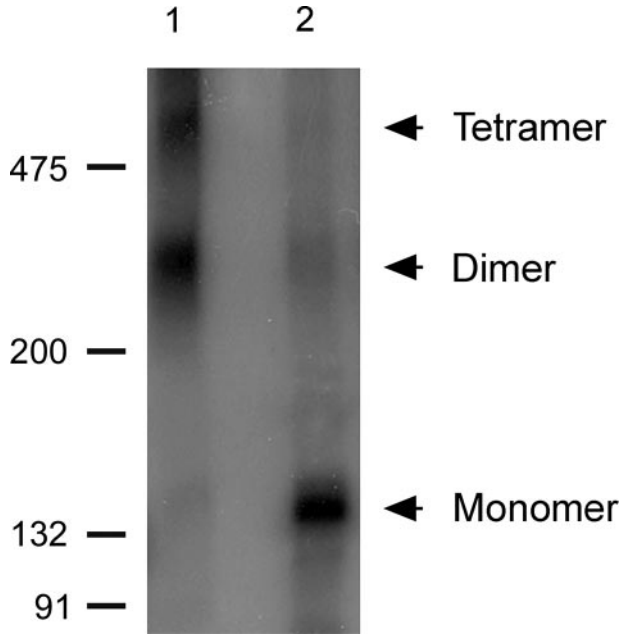

FIGURE 5. **Covalent cross-linking of membrane-embedded NBCe1-A proteins expressed in HEK293 cells with *N*-hydroxysuccinimide ester (BS^3).** Membrane proteins cross-linked with BS^3 (*lane 1*) and not cross-linked (*lane 2*) were analyzed by SDS-PAGE and immunoblotting in the presence of DTT. The immunoblots were probed with an anti-NBCe1-A antibody.

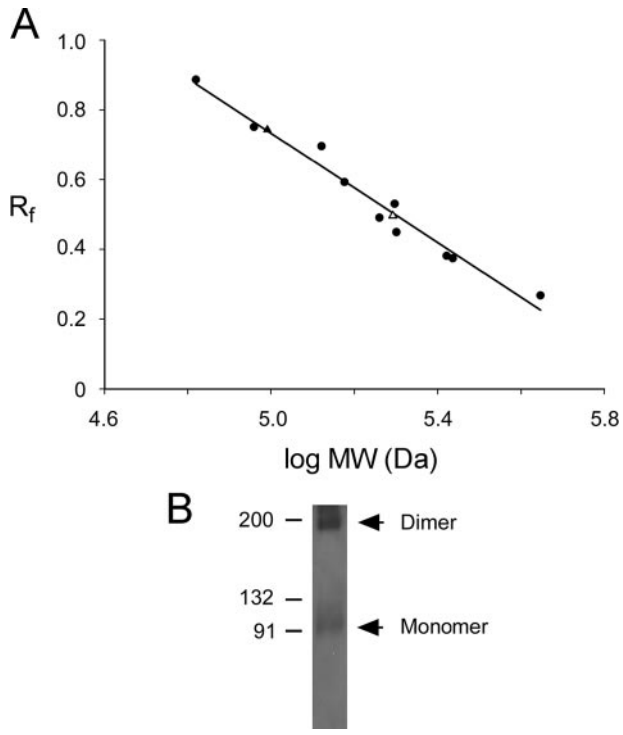

FIGURE 6. **Determination of the molecular mass of NBCe1-A by 7.5% PFO-PAGE.** *A,* calibration curve was generated using standards of known molecular mass (*closed circles*). To confirm the fidelity of the standardized PFO-polyacrylamide gel to estimate the molecular mass of membrane proteins, the curve was used to predict the molecular mass of AE1 monomer (*open triangle*) and dimer (*closed triangle*). The estimated molecular mass of AE1 monomer and dimer was 98.6 ± 0.5 kDa ($n = 4$) and 198.0 ± 3.0 kDa ($n = 4$), respectively. The molecular mass of NBCe1-A monomer and dimer was 143.2 ± 2.1 kDa ($n = 4$) and 291.4 ± 1.3 kDa ($n = 4$), respectively. *B,* bovine red blood cell ghost sample run on PFO-PAGE in the presence of DTT, and immunoblots were probed with a previously characterized anti-AE1 antibody kindly provided by Dr. Inaba (81). Note that unlike NBCe1-A, AE1 retains its oligomeric structure in the presence of DTT using PFO-PAGE analysis.

Downloaded from www.jbc.org by guest, on September 29, 2009

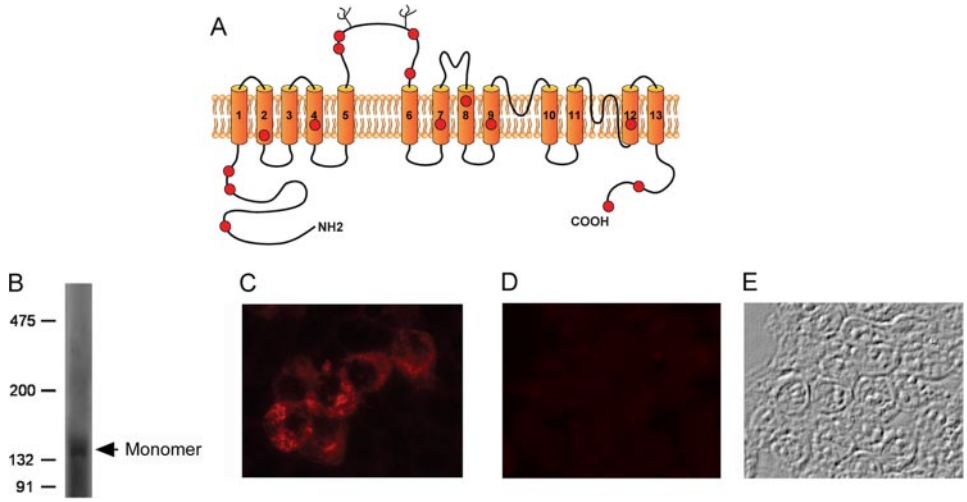

FIGURE 7. *A,* putative topology of NBCe1-A based on the AE1 membrane domain topology model by Zhu and Casey (23). NBCe1-A possesses 15 cysteine residues, which could form S–S bonds that play a role in the oligomerization of the cotransporter. *B,* PFO-PAGE analysis of the cysteineless NBCe1-A mutant in the absence of DTT. *C,* immunocytochemistry of HEK293 cells expressing the NBCe1-A cysteineless mutant stained with the anti-NBCe1-A antibody. *D,* immunocytochemistry of mock-transfected HEK293 cells stained with the anti-NBCe1-A antibody. *E,* Nomarski image of the cells in *D*.

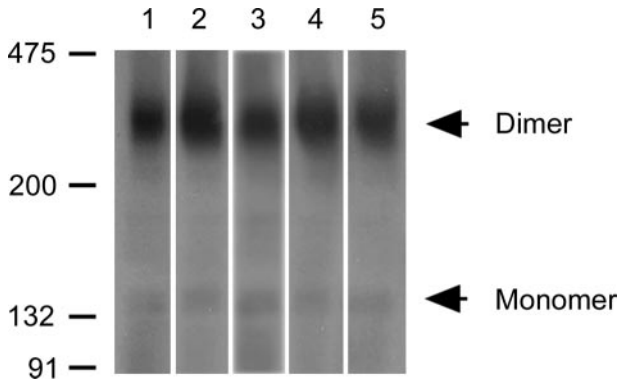

FIGURE 8. **GXXXG motif and oligomerization of NBCe1-A.** Each of the five G*XXX*G wild-type residues was mutated to a Ser, and the effect of oligomerization on the cotransporter was assessed. Using the nondenaturing detergent PFO in the absence of DTT, all NBCe1-A constructs were able to form stable oligomers. *Lane 1,* G444S; *lane 2,* G445S; *lane 3,* L446S; *lane 4,* L447S; *lane 5,* G448S.

NBCe1-A dimers, or an NBCe1-A heterocomplex. As in the mouse kidney, only a weak band corresponding to the monomeric form of the cotransporter was detected. In the presence of DTT, only the monomeric form of NBCe1-A expressed in HEK293 cells was detected. Therefore, NBCe1-A is also expressed in HEK293 cells predominantly as a dimer. The relative amount of dimeric *versus* tetrameric and monomeric forms of the cotransporter is shown in Fig. 4*B*.

The results suggest that S–S bonds are involved in the oligomerization of the cotransporter. We also performed cross-linking experiments on plasma membrane NBCe1-A expressed in HEK293 cells to capture the oligomeric state of the cotransporter in living cells prior to performing the immunoblotting experiments (40). In these experiments, covalent cross-linking of NBCe1-A was performed using extracellular BS^3. A major band likely corresponding to a dimer and a less intense higher order oligomer that likely corresponds to the tetrameric form were detected after cross-linking (Fig. 5). Monomers were essentially undetectable. As shown in Fig. 5 unlike cells not exposed to BS^3, following cross-linking of NBCe1-A with BS^3, the oligomers were resistant to DTT. These results confirmed the data obtained using PFO and indicate that NBCe1-A monomers are a maximum distance of 11.4 Å based on the length of the cross-linker.

Determination of the Molecular Mass of NBCe1-A—The molecular mass of the NBCe1-A oligomer was deduced under nondenaturing conditions (Fig. 6). A molecular mass calibration curve for a 7.5% PFO-polyacrylamide gel was constructed from migration distances of specific proteins with known molecular masses as described previously (40). As shown in Fig. 6*A*, the migration of the protein standards fit a log-linear molecular mass-R_F relation indicating that the proteins are adequately separated based on their molecular mass. To confirm the fidelity of the standardized PFO-polyacrylamide gel to estimate the molecular mass of membrane proteins, we further assessed the mobility of AE1, given that it is the most structurally characterized member of the SLC4 family and shares a sequence homology to NBCe1-A (Fig. 6*B*) (41–46). Using the standard curve in Fig. 6*A*, the value of the molecular mass of the monomeric form of AE1 was 98.6 ± 0.5 kDa ($n = 4$) and dimeric form was 198.0 ± 3.0 kDa ($n = 4$) as reported previously (43, 45, 46). As shown in Fig. 6, the estimated apparent molecular mass of the NBCe1-A monomer and dimer (the predominant oligomeric form of the cotransporter) were predicted to be 143.2 ± 2.1 kDa ($n = 4$) and 291.4 ± 1.3 kDa ($n = 4$), respectively.

Role of Cysteine Residues in the Oligomerization of NBCe1-A—NBCe1-A possesses 15 cysteine residues, which could form S–S bonds that play a role in the oligomerization of the cotransporter (Fig. 7*A*). As shown earlier, wt-NBCe1-A oligomers are split into monomers by DTT suggesting that S–S bonds play an important role in its stabilizing NBCe1-A oligomers. Accordingly, it would be predicted that in the absence of native cysteine residues, NBCe1-A would not form stable oligomers. To address this question, we determined whether a cysteineless NBCe1-A mutant could form dimers and/or higher order oligomers. Under nondenaturing conditions as shown in Fig. 7*B* in the absence of DTT, the cysteineless mutant was monomeric and was expressed unlike the wild-type cotransporter in the cytoplasm (Fig. 7*C*). These findings confirm the previous results with DTT, and indicate the following: 1) S–S bonds are essential for NBCe1-A to form stable oligomers; and 2) S–S bonds are the only mechanism for covalent attachment of NBCe1-A monomers.

Lack of a Role of GXXXG Motif in Interhelical Hydrogen Bonding of NBCe1-A Monomers—SLC4 transporters have a GGLLG sequence (residues 444–448 in NBCe1-A) that corresponds to a G*XXX*G or GG4 motif that plays an important role in helix-

Downloaded from www.jbc.org by guest, on September 29, 2009

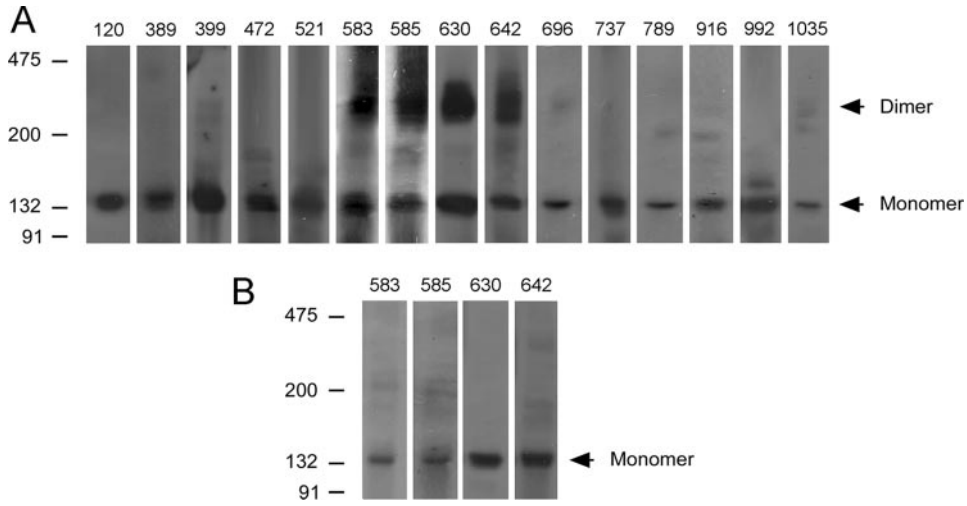

FIGURE 9. *A,* oligomeric structure of 15 NBCe1-A mutants containing single individual native cysteine residues added to a cysteineless NBCe1-A backbone analyzed under nondenaturing conditions in the absence of DTT. *B,* oligomeric structure of mutants NBCe1-A-Cys^{583}, NBCe1-A-Cys^{585}, NBCe1-A-Cys^{630}, and NBCe1-A-Cys^{642} under nondenaturing conditions in the presence of DTT. *A* and *B*, *number* at the *top* of each lane refers to the position of cysteine residue remaining in the construct.

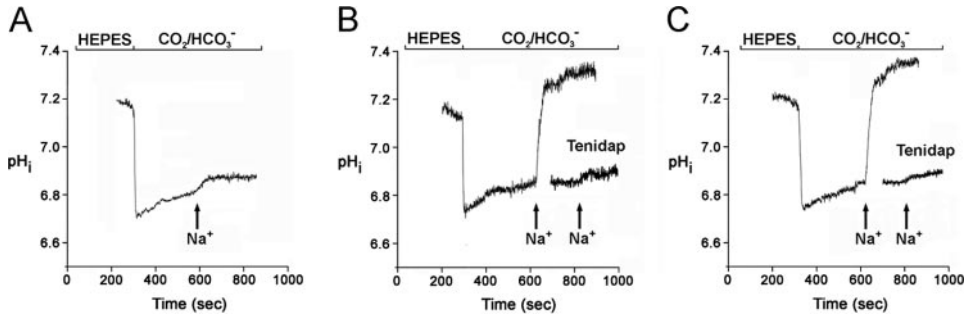

FIGURE 10. **Representative experiment showing the function of NBCe1-A-Cys^{992} mutant.** *A,* mock-transfected cells; *B,* wt-NBCe1-A; and *C,* NBCe1-A-Cys^{992} mutant. *A–C*, cells were initially bathed in a HEPES-buffered solution in the absence of Na^+. Where indicated, the solution was switched to an HCO_3^--buffered zero-Na^+ containing solution. The flux through NBCe1-A (wild-type and mutant constructs) was assayed following the addition of a Na^+-containing HCO_3^--buffered solution. Separate experiments using the identical protocol were performed in the presence of the NBCe1-A inhibitor Tenidap (0.2 mM (82); kindly provided by Vladimir Maslenko). See Table 1 for a summary of all cysteine mutants generated on a cysteineless backbone.

TABLE 1

Function of NBCe1-A constructs with a single remaining native cysteine residue

Cysteine residue	pH_i (Na^+ addition)	Equivalent base flux	Equivalent base flux (% wt-NBCe1-A)
			mM/min
Cys^{120}	6.84 ± 0.03	13 ± 1[a]	66 ± 5[a]
Cys^{389}	6.84 ± 0.03	12 ± 2[a]	59 ± 9[a]
Cys^{399}	6.86 ± 0.03	17 ± 2[a]	79 ± 7[a]
Cys^{472}	6.81 ± 0.02	16 ± 2[a]	76 ± 7[a]
Cys^{521}	6.85 ± 0.02	10 ± 1[a]	49 ± 3[a]
Cys^{583}	6.78 ± 0.03	0 ± 0[a]	0[a]
Cys^{585}	6.76 ± 0.01	2.0 ± 0.2[a]	9 ± 1[a]
Cys^{630}	6.82 ± 0.01	6.1 ± 1[a]	29 ± 5[a]
Cys^{642}	6.79 ± 0.02	9.1 ± 2[a]	44 ± 7[a]
Cys^{696}	6.84 ± 0.02	18 ± 2[a]	86 ± 9[a]
Cys^{737}	6.77 ± 0.01	8.5 ± 1[a]	40 ± 3[a]
Cys^{789}	6.79 ± 0.04	5.5 ± 1[a]	25 ± 3[a]
Cys^{916}	6.81 ± 0.04	3.4 ± 0.2[a]	16 ± 1[a]
Cys^{992}	6.83 ± 0.03	20 ± 2	95 ± 6
Cys^{1035}	6.82 ± 0.05	15 ± 2[a]	70 ± 7[a]

[a] $p < 0.05$ *versus* wt-NBCe1-A flux (equivalent base flux) of 21 ± 2 mM/min (Dunnett's *t* test). Five or more experiments were done for each construct.

helix dimerization of glycophorin A and the oligomerization of other proteins (47, 48). Interaction between glycine residues stabilizes oligomers by forming interhelical hydrogen bond. Interhelical hydrogen bonding between NBCe1-A monomers could therefore play an important role in stabilizing the NBCe1-A monomers prior to S–S bond formation in the endoplasmic reticulum lumen. To determine whether the G*XXX*G motif in NBCe1-A is a necessary requirement for stabilizing NBCe1-A oligomers, each of the residues in the GGLLG sequence was mutated individually to a serine residue, and their ability to oligomerize was examined. As shown in Fig. 8, all constructs were able to form stable oligomers under nondenaturing conditions. These results indicate that stable oligomerization of the cotransporter is not dependent on the GG4 motif.

Cysteine Mutants—NBCe1-A has 15 native cysteine residues (Fig. 7*A*) that could contribute to S–S bond formation (*a*) within a given monomer and/or (*b*) between individual monomers. Only the latter process can contribute to the formation of stable NBCe1-A oligomers via S–S bond formation. We generated 15 NBCe1-A mutants containing single individual native cysteine residues that were added onto a cysteineless backbone, and each construct was expressed in HEK293 cells. Of the constructs studied, four mutants were able to form S–S bonded dimers (Fig. 9) as follows: NBCe1-A-Cys^{583}, NBCe1-A-Cys^{585}, NBCe1-A-Cys^{630}, and NBCe1-A-Cys^{642}. All four cysteine residues are in putative extracellular loop 3 (Fig. 7). NBCe1-A-Cys^{992} mutant was also of particular interest because although stable monomers linked by an S–S bond were not formed, the function of this construct was not different from that of wt-NBCe1-A (Fig. 10 and Table 1). Representative experiments are shown in Fig. 10 where the mean functional activity of the NBCe1-A-Cys^{992} mutant was 20 ± 2 mM/min, $n = 9$ (p = not significant *versus* the wt-NBCe1-A). These data indicate the following: 1) S–S bonds between NBCe1-A monomers are not a necessary requirement for functional activity, and 2) the cysteine residues in extracellular loop 3 do not play an essential functional role.

Given that one or more of the cysteine residues in extracellular loop 3 is capable of mediating the formation of stable oligomers in the context of an otherwise cysteineless backbone, in separate experiments, individual cysteine residues were removed from a wt-NBCe1-A backbone to determine whether a single S–S bond mediated by one of the four cysteine residues in extracellular loop 3 was involved in intermonomeric S–S bonding. As shown in Fig. 11*A*, none of the individual cysteine

Downloaded from www.jbc.org by guest, on September 29, 2009

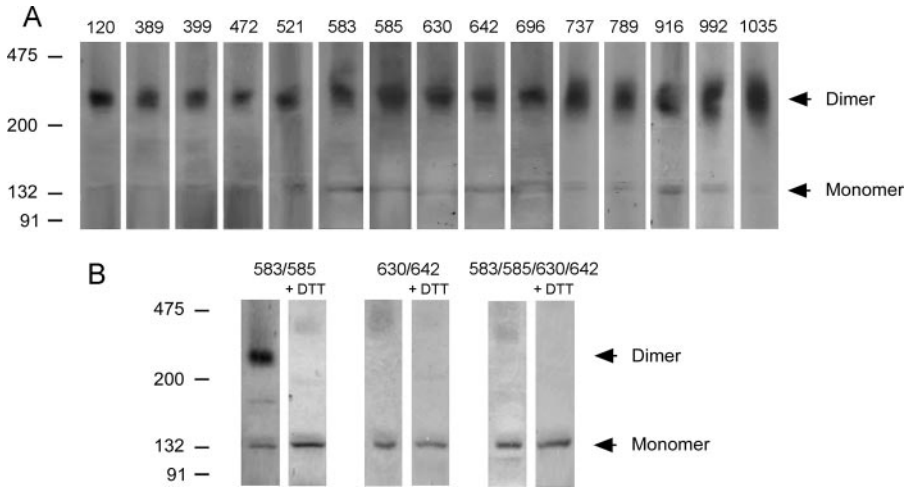

FIGURE 11. *A,* oligomeric structure of 15 NBCe1-A mutants containing single individual native cysteine residues removed from the wt-NBCe1-A backbone analyzed under nondenaturing conditions in the absence of DTT. *B,* oligomeric structure of the NBCe1-A 583/585, 630/642, and 583/585/630/642 mutants in the absence and presence of DTT.

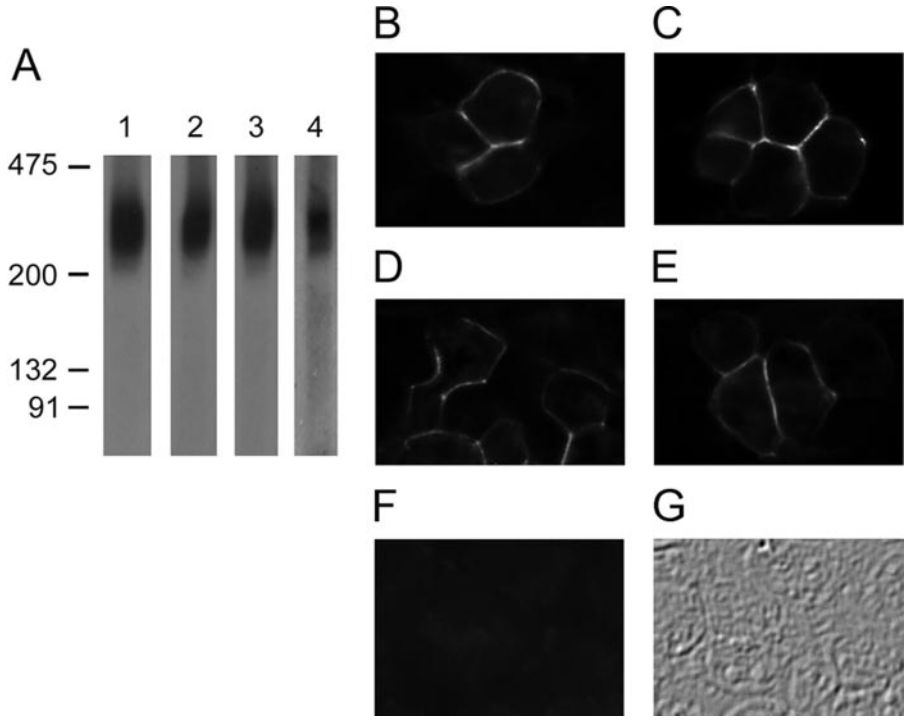

FIGURE 12. **Concatameric constructs of wt-NBCe1-A and NBCe1-A^{T442C} mutant to determine the minimal functional unit of the cotransporter.** Four concatameric constructs were made as follows: *1,* wt-NBCe1-A-linker-wt-NBCe1-A; *2,* wt-NBCe1-A-linker-NBCe1-A^{T442C}; *3,* NBCe1-A^{T442C}-linker-wt-NBCe1-A; and *4,* NBCe1-A^{T442C}-linker-NBCe1-A^{T442C}. The linker consisted of a Gly-Ser pair. *A,* PFO-PAGE analysis of concatameric constructs: wt-NBCe1-A-linker-wt-NBCe1-A (*lane 1*); wt-NBCe1-A-linker-NBCe1-A^{T442C} (*lane 2*); NBCe1-A^{T442C}-linker-wt-NBCe1-A (*lane 3*); and NBCe1-A^{T442C}-linker-NBCe1-A^{T442C} (*lane 4*). As shown, the estimated molecular mass of each concatameric construct was twice the molecular mass of wt-NBCe1-A monomers. *B–E,* immunocytochemistry of each concatameric construct stained with the anti-NBCe1-A antibody; *B,* wt-NBCe1-A-linker-wt-NBCe1-A; *C,* wt-NBCe1-A-linker-NBCe1-A^{T442C}; *D,* NBCe1-A^{T442C}-linker-wt-NBCe1-A, and *E,* NBCe1-A^{T442C}-linker-NBCe1-A^{T442C} expressed in HEK293 cells. *F,* immunocytochemistry of mock-transfected HEK293 cells stained with the anti-NBCe1-A antibody. *G,* Nomarski image of the cells in *F*.

residues when removed from a wt-NBCe1-A backbone prevented stable dimerization of the cotransporter. These data indicate that more than one S–S bond must mediate the stable oligomerization of the cotransporter likely involving two or more cysteine residues in putative extracellular loop 3. Therefore, additional experiments were done where cysteine residues in extracellular loop3 were mutated. The results shown in Fig. 11*B* indicated that Cys^{630} and Cys^{642} form S–S bonds between NBCe1-A monomers.

NBCe1-A Minimal Functional Unit—The previous data indicated that stable S–S bonded NBCe1-A is not a requirement for cotransporter function. In the following experiments, we therefore addressed the question as to whether individual monomers within the NBCe1-A oligomer are functional. We recently reported that an NBCe1-A^{T442C} mutant functions normally and that the flux through the mutant cotransporter unlike wt-NBCe1-A is completely inhibited by MTS reagents (49). This mutant could therefore be used in concert with wt-NBCe1-A to help identify the functional unit of the cotransporter. One approach to identifying the functional unit of NBCe1-A is to coexpress plasmid DNA encoding wt-NBCe1-A and the T442C mutant and to determine the percent functional inhibition using MTS reagents. This approach requires the following: 1) both wt-NBCe1-A and the T442C mutant are expressed independently, and 2) the membrane expression levels correspond to a given quantity of plasmid DNA transfected and expressed. If the two cotransporters associate randomly to form functional oligomeric complexes, using the binomial theorem, one can predict the magnitude of functional inhibition with MTS reagents and the proportion of each cotransporter that is expressed. However, given the aforementioned assumptions and uncertainties involved, we elected to utilize a concatameric approach. This method was first utilized with voltage-gated K^+ channels (50) and has since been applied to analyze other membrane proteins, including aquaporins (51), the Na^+,K^+-ATPase (52), ligand-gated ion channels (53), lactose permease (54), NaP_i2 (55), KAAT1 (56), and CAATCH1 (56). The following concatameric constructs of wt-NBCe1-A and NBCe1-A^{T442C} were analyzed by immunoblotting, immunocytochemistry, and functionally the following: 1) wt-NBCe1-A-linker-wt-NBCe1-A used as a negative con-

Downloaded from www.jbc.org by guest, on September 29, 2009

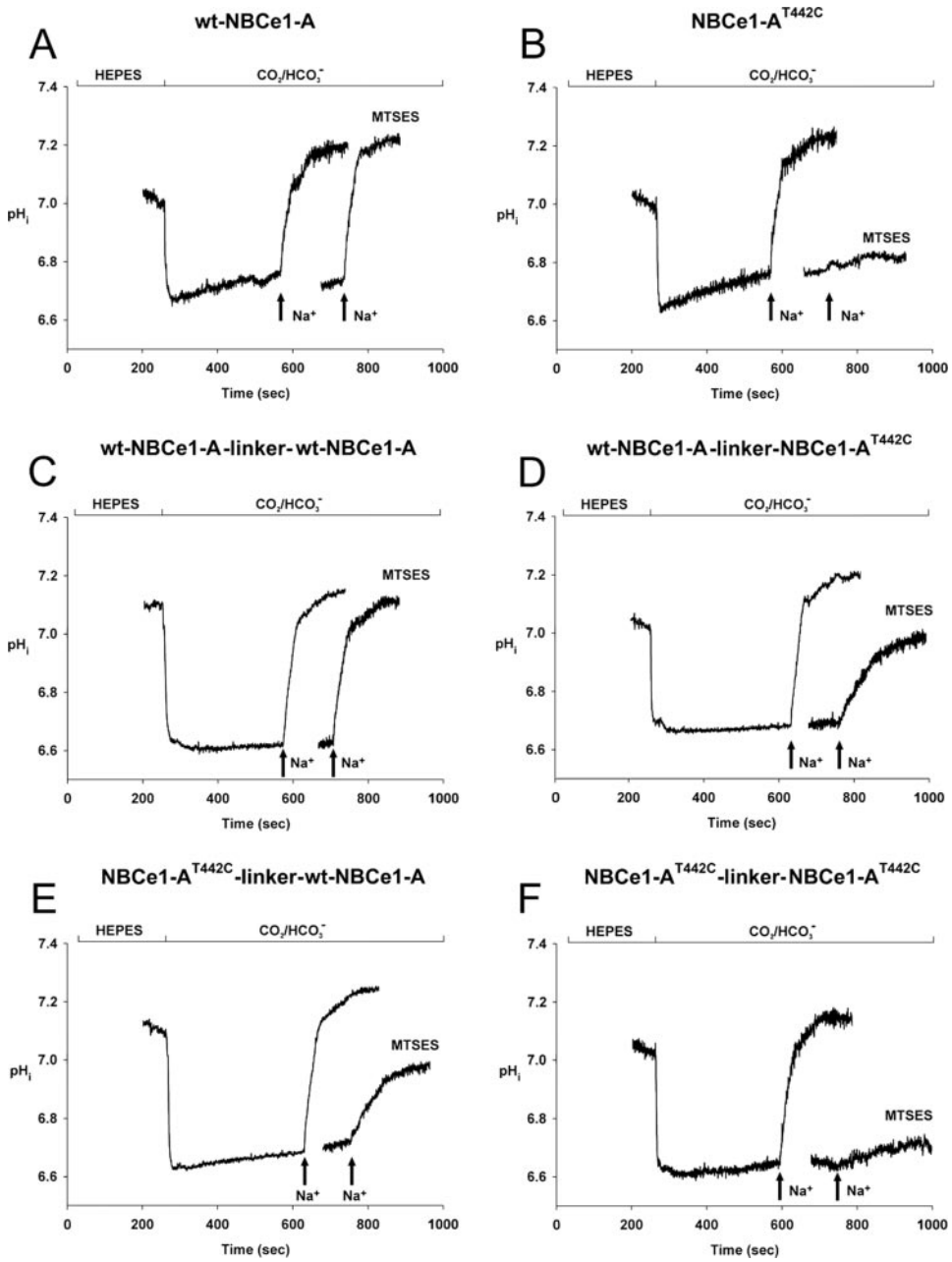

FIGURE 13. **Representative experiments depicting the following function.** *A,* wt-NBCe1-A; *B;* NBCe1-A^{T442C} and the four concatamers (*C–F*). *C,* wt-NBCe1-A-linker-wt-NBCe1-A; *D,* wt-NBCe1-A-linker-NBCe1-A^{T442C}; *E,* NBCe1-A^{T442C}-linker-wt-NBCe1-A; and *F* NBCe1-A^{T442C}-linker-NBCe1-A^{T442C} in the presence or absence of MTSES.

trol; 2) wt-NBCe1-A-linker-NBCe1-A^{T442C}; 3) NBCe1-A^{T442C}-linker-wt-NBCe1-A; and 4) NBCe1-A^{T442C}-linker-NBCe1-A^{T442C} used as a positive control. As shown in Fig. 12*A*, under nondenaturing conditions, each construct was expressed at the predicted size of dimers of NBCe1-A demonstrating that both halves of each concatamer were expressed properly. In addition as shown in Fig. 12, *B–E*, each concatamer was targeted to the plasma membrane. As shown in Fig. 13 and Fig. 14, the function of the four concatamers was similar to wt-NBCe1-A and NBCe1-A^{T442C}. In the presence of the MTS reagent MTSES (4 mM), the function of both mixed concatamers (wt-NBCe1-A-linker-NBCe1-A^{T442C} and NBCe1-A^{T442C}-linker-wt-NBCe1-A) was decreased to ~50% of normal. The function of the wt-NBCe1-A homo-concatamer was unaffected, whereas MTSES blocked the function of the mutant NBCe1-A^{T442C} homo-concatamer. The results indicate that individual NBCe1-A monomers are functional.

DISCUSSION

In this study, we report for the first time studies that have characterized the oligomeric state of wt-NBCe1-A and have determined the minimal functional unit of the cotransporter. Our experiments show that native NBCe1-A is an oligomer in mouse kidney and also when the cotransporter is expressed heterologously in HEK293 cells. The predominant oligomeric state of the cotransporter is dimeric, although higher order oligomers (dimers of dimers or tetramers) are also present to a lesser extent. The oligomerization of NBCe1-A is mediated by covalent S–S bonds that are formed between monomeric subunits. NBCe1-A therefore differs structurally from AE1, which forms stable dimers in the absence of S–S bond formation. Importantly, although NBCe1-A forms a structural oligomer, each monomeric subunit maintains its own independent transport activity.

The oligomerization state of most transporters in the SLC4 family is currently unknown, with the exception of AE1 (8, 57) and brain AE3 (28). Depending on the detergent used for solubilization and temperature, AE1 was shown to be predominantly a monomer, dimer, or tetramer (26, 41, 42, 45). AE1 dimers were shown to be arranged in two-dimensional crystals in higher order units characterized by 3-fold symmetry (57). Transmission electron microscopy studies of bAE3 purified by immunoaffinity chromatography from rabbit kidney revealed predominantly AE3 tetramers (28). Because both AE1 and AE3 transport chloride in exchange for bicarbonate, our current results represent the first detailed study of the oligomerization of a sodium-dependent bicarbonate cotransport of the SLC4 family. Moreover, NBCe1-A is the first member of the SLC4 family whose stable oligomerization has been shown to be dependent on disulfide bond formation. In this way, the

Downloaded from www.jbc.org by guest, on September 29, 2009

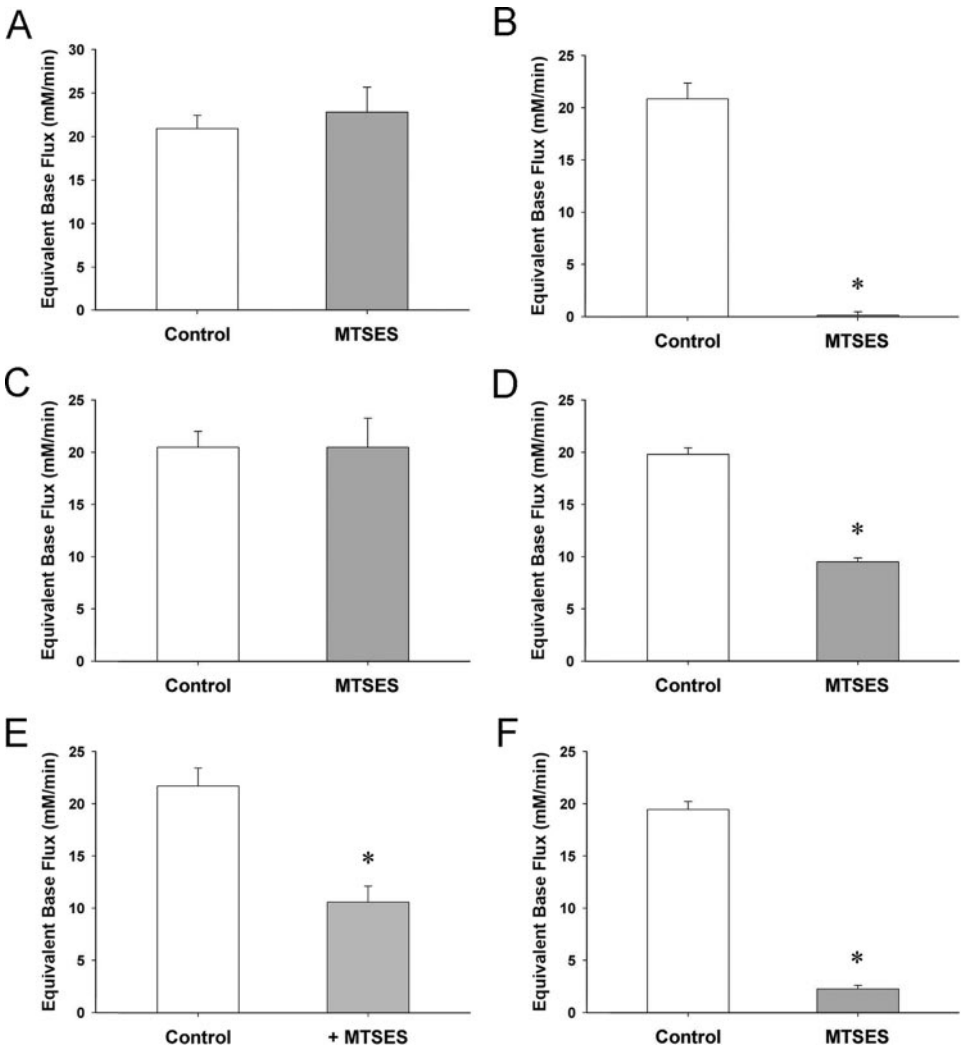

FIGURE 14. **Summary data demonstrating the following functional activities.** *A,* wt-NBCe1-A; *B,* NBCe1-A^{T442C} and the four concatamers (*C–F*). *C,* wt-NBCe1-A-linker-wt-NBCe1-A; *D,* wt-NBCe1-A-linker-NBCe1-A^{T442C}; *E,* NBCe1-A^{T442C}-linker-wt-NBCe1-A; and *F,* NBCe1-A^{T442C}-linker-NBCe1-A^{T442C} in the presence or absence of MTSES.

cotransporter differs from AE1 whose oligomerization occurs independent of the potential reduction of S–S bonds (44).

In this study, we used the nondenaturing detergent PFO for determining the oligomeric state of NBCe1-A. PFO is a novel detergent that is known to protect the interactions between monomers in oligomeric membrane proteins and has been used in various studies to evaluate the mass and quaternary structure of membrane proteins such as claudin-4, ABCG2, the vanilloid receptor, and prestin (40, 58–60). Our experiments under denaturing and nondenaturing conditions demonstrate that both the dimeric and tetrameric (or dimer of dimer) variants of NBCe1-A are converted into monomers in the presence of DTT. Given that DTT was capable of completely splitting all NBCe1-A oligomers into monomers, other than S–S bonds, there does not appear to be any other significant mechanism for covalent bond formation between NBCe1-A monomers as has been reported, for example, in regard to the AT_1 receptor (61). In addition, our findings suggest that NBCe1-A monomers in the absence of S–S bonding lack strong noncovalent electrostatic/hydrophobic interactions under nondenaturing conditions that can maintain their initial oligomeric state. Finally, our results demonstrate that the interaction between NBCe1-A and AE1 monomers is fundamentally different in that AE1 monomers form stable oligomers in a nondenaturing detergent under reducing conditions. These findings suggest that AE1 oligomerization is dependent on strong noncovalent electrostatic/hydrophobic interactions rather than covalent S–S bond formation (26).

The apparent molecular mass of the NBCe1-A monomer and dimer was ~143 and 291 kDa using PFO-PAGE methodology (31, 40). Because soluble proteins and membrane proteins can differ in their mobility in the PFO-PAGE system, the molecular masses obtained by PFO-PAGE analysis must be regarded as relative values rather than absolute. The errors introduced by this approach do not appear to be too great, however, given that by using the calibration curve shown in Fig. 6*A*, we were able to accurately estimate the molecular mass of the related SLC4 membrane protein AE1 monomer as ~99 kDa and the dimer as ~198 kDa.

Cysteine residues are known to form intra-monomeric disulfide and/or inter-monomeric S–S bonds thereby stabilizing a protein's folded confirmation (62–68). In the absence of all native cysteine residues, NBCe1-A monomers are retained intracellularly presumably because of abnormal folding of the protein (63, 64, 69, 70). In addition, the importance of S–S bond formation in mediating the oligomerization of membrane proteins as a requirement for normal transport function has been shown for sodium-dependent neurotransmitter transporters (71), SGLT1 (72), and for the oligomerization of mouse and human resistins (73), E-cadherin (74), and hyaluronan-binding protein 1 (75).

Our data rule out a requirement for intramonomeric S–S bond formation as being an absolute requirement for normal NBCe1-A function. Specifically, when Cys^{992} was introduced into the cysteineless mutant, functional activity was normal. In these experiments, because all the native cysteine residues other than Cys^{992} were absent, Cys^{992} in a given monomer could theoretically only form a disulfide bond with a second monomer. However, the Cys^{992} mutant lacked an S–S bond unlike the wild-type transporter, which is presumably because of the cytoplasmic localization Cys^{992} that precludes Cys^{992}

Downloaded from www.jbc.org by guest, on September 29, 2009

from mediating S–S bonding in either the mutant or wild-type transporter.

Of the 15 native cysteine residues, our data suggest that Cys^{630} and Cys^{642} in extracellular loop 3 are involved in the formation of S–S bonds between NBCe1-A monomers. None of the cysteine residues outside of extracellular loop 3 formed S–S bonded oligomers. These findings are compatible with the fact that intracellular cysteine residues (N-terminal Cys^{120}, Cys^{389}, and Cys^{399}, and C-terminal Cys^{992} and Cys^{1035}) would not be expected to form S–S bonds because of the reducing environment in the cytoplasm (76, 77). Moreover, cysteine residues in transmembrane regions are in general in a nonaqueous environment (unless a given residue resides in an aqueous pore) and would also not be expected to be involved in S–S bond formation.

Although NBCe1-A is structurally an oligomer dependent on S–S bond formation, our results provide the first demonstration that individual NBCe1-A monomers are functional. Taking advantage of the specific inhibition of the NBCe1-A^{T442C} by MTS reagents (49), we used a concatameric approach to investigate the minimal functional unit of the cotransporter. These studies confirmed that individual NBCe1-A monomers in the cotransporter dimer are functional. From our data, we cannot rule out, however, whether additional ion permeation pathways are created by the formation of NBCe1-A dimers and tetramers. This possibility is suggested by the recent preliminary data of Chang *et al.* (78) who reported that in oocytes transfected with nonfunctional NBCe1-A mutants, functional cotransporter activity can be detected. The latter findings suggest that oligomerization of nonfunctional mutant monomers can create a functional ion permeation pathway. Whether these findings hold true in the context of wild-type monomer oligomerization is unknown. The results we obtained using NBCe1-A concatamers suggest that the function of monomeric NBCe1-A is similar to the wild-type cotransporter. Whether more subtle differences in ion affinity and permeation characterize the different oligomeric states of the cotransporter requires further studies.

Both in kidney and in HEK293 cells expressing the cotransporter, the ratio of NBCe1-A dimers in comparison with monomers and higher order oligomers (consisting of tetramers or dimers of dimers) is favored thermodynamically by a factor of 5:1 and 2.5:1, respectively. Other transport proteins known to be oligomers whose transport behavior is consistent with activity as monomers include lactose, permease (54), AE1 (79), aquaporin-1 (51), NKCC2 (80), KAAT1 (56), and CAATCH1 (56). An obvious question then arises from these studies and our data. Given that monomers are functional in NBCe1-A and the aforementioned transporters, what are the selective biological advantages for functional monomers to assemble as oligomers? Although conjectural given our present state of knowledge, oligomerization may provide a selective advantage in altering plasma membrane half-life and stability and modulating the dynamics of protein/protein interactions in the plasma membrane.

Currently, all mutations in NBCe1 are inherited in an autosomal recessive pattern. In contrast, mutations in AE1 cause distal renal tubular acidosis that can be inherited in a dominant or recessive manner (9–12). In autosomal dominant AE1 mutations, dimers containing a mixed wild-type and mutant monomer are targeted to the endoplasmic reticulum-associated degradation pathway presumably because of lack of acquisition of a native conformation (12). Mutations in AE1 inherited in a recessive manner are expressed normally on the plasma membrane with the functional monomer in the mixed dimer still able to transport normally (12). The finding that NBCe1-A is predominantly a dimer composed of functional monomers leads to the interesting prediction that in the known mixed mutant-wild-type dimers (heterozygotes; parents of patients with autosomal recessive NBCe1-A-mediated proximal renal tubular acidosis), the wild-type monomer is functional, and the mutant monomer is not capable of targeting the mixed dimer to the endoplasmic reticulum-associated degradation pathway resulting in the lack of a significant phenotype. To address this issue more precisely, an understanding of the specific residues involved in coordinating the electrostatic/hydrophobic interaction between monomers prior to S–S bond formation will play an important role in future studies involving the biosynthesis of NBCe1-A.

REFERENCES

1. Donckerwolcke, R. A., van Stekelenburg, G. J., and Tiddens, H. A. (1970) *Arch. Dis. Child* **45,** 769–773
2. Igarashi, T., Ishii, T., Watanabe, K., Hayakawa, H., Horio, K., Sone, Y., and Ohga, K. (1994) *Pediatr. Nephrol.* **8,** 70–71
3. Lemann, J., Jr., Adams, N. D., Wilz, D. R., and Brenes, L. G. (2000) *Kidney Int.* **58,** 1267–1277
4. Winsnes, A., Monn, E., Stokke, O., and Feyling, T. (1979) *Acta Paediatr. Scand.* **68,** 861–868
5. Igarashi, T., Inatomi, J., Sekine, T., Cha, S. H., Kanai, Y., Kunimi, M., Tsukamoto, K., Satoh, H., Shimadzu, M., Tozawa, F., Mori, T., Shiobara, M., Seki, G., and Endou, H. (1999) *Nat. Genet.* **23,** 264–266
6. Romero, M. F., Hediger, M. A., Boulpaep, E. L., and Boron, W. F. (1997) *Nature* **387,** 409–413
7. Gawenis, L. R., Bradford, E. M., Prasad, V., Lorenz, J. N., Simpson, J. E., Clarke, L. L., Woo, A. L., Grisham, C., Sanford, L. P., Doetschman, T., Miller, M. L., and Shull, G. E. (2007) *J. Biol. Chem.* **282,** 9042–9052
8. Pushkin, A., and Kurtz, I. (2006) *Am. J. Physiol.* **290,** F580–F599
9. Bruce, L. J., Cope, D. L., Jones, G. K., Schofield, A. E., Burley, M., Povey, S., Unwin, R. J., Wrong, O., and Tanner, M. J. (1997) *J. Clin. Investig.* **100,** 1693–1707
10. Jarolim, P., Shayakul, C., Prabakaran, D., Jiang, L., Stuart-Tilley, A., Rubin, H. L., Simova, S., Zavadil, J., Herrin, J. T., Brouillette, J., Somers, M. J., Seemanova, E., Brugnara, C., Guay-Woodford, L. M., and Alper, S. L. (1998) *J. Biol. Chem.* **273,** 6380–6388
11. Karet, F. E., Gainza, F. J., Gyory, A. Z., Unwin, R. J., Wrong, O., Tanner, M. J., Nayir, A., Alpay, H., Santos, F., Hulton, S. A., Bakkaloglu, A., Ozen, S., Cunningham, M. J., di Pietro, A., Walker, W. G., and Lifton, R. P. (1998) *Proc. Natl. Acad. Sci. U. S. A.* **95,** 6337–6342
12. Kittanakom, S., Cordat, E., Akkarapatumwong, V., Yenchitsomanus, P. T., and Reithmeier, R. A. (2004) *J. Biol. Chem.* **279,** 40960–40971
13. Sander, T., Toliat, M. R., Heils, A., Leschik, G., Becker, C., Ruschendorf, F., Rohde, K., Mundlos, S., and Nurnberg, P. (2002) *Epilepsy Res.* **51,** 249–255
14. Hentschke, M., Wiemann, M., Hentschke, S., Kurth, I., Hermans-Borgmeyer, I., Seidenbecher, T., Jentsch, T. J., Gal, A., and Hubner, C. A. (2006) *Mol. Cell. Biol.* **26,** 182–191
15. Bok, D., Galbraith, G., Lopez, I., Woodruff, M., Nusinowitz, S., Beltrandel-Rio, H., Huang, W., Zhao, S., Geske, R., Montgomery, C., Van Sligtenhorst, I., Friddle, C., Platt, K., Sparks, M. J., Pushkin, A., Abuladze, N., Ishiyama, A., Dukkipati, R., Liu, W., and Kurtz, I. (2003) *Nat. Genet.* **34,** 313–319
16. Barkley, R. A., Chakravarti, A., Cooper, R. S., Ellison, R. C., Hunt, S. C., Province, M. A., Turner, S. T., Weder, A. B., and Boerwinkle, E. (2004)

Downloaded from www.jbc.org by guest, on September 29, 2009

Hypertension **43,** 477–482
17. Desir, J., Moya, G., Reish, O., Van Regemorter, N., Deconinck, H., David, K. L., Meire, F. M., and Abramowicz, M. J. (2007) *J. Med. Genet.* **44,** 322–326
18. Vithana, E. N., Morgan, P. E., Ramprasad, V., Tan, D. T., Yong, V. H., Venkataraman, D., Venkatraman, A., Yam, G. H., Nagasamy, S., Law, R. W., Rajagopal, R., Pang, C. P., Kumaramanickevel, G., Casey, J. R., and Aung, T. (2008) *Hum. Mol. Genet.* **17,** 656–666
19. Vithana, E. N., Morgan, P., Sundaresan, P., Ebenezer, N. D., Tan, D. T., Mohamed, M. D., Anand, S., Khine, K. O., Venkataraman, D., Yong, V. H., Salto-Tellez, M., Venkatraman, A., Guo, K., Hemadevi, B., Srinivasan, M., Prajna, V., Khine, M., Casey, J. R., Inglehearn, C. F., and Aung, T. (2006) *Nat. Genet.* **38,** 755–757
20. Aldave, A. J., Yellore, V. S., Bourla, N., Momi, R. S., Khan, M. A., Salem, A. K., Rayner, S. A., Glasgow, B. J., and Kurtz, I. (2007) *Cornea* **26,** 896–900
21. Choi, I., Hu, L., Rojas, J. D., Schmitt, B. M., and Boron, W. F. (2003) *Am. J. Physiol.* **284,** F1199–F1206
22. Tatishchev, S., Abuladze, N., Pushkin, A., Newman, D., Liu, W., Weeks, D., Sachs, G., and Kurtz, I. (2003) *Biochemistry* **42,** 755–765
23. Zhu, Q., and Casey, J. R. (2004) *J. Biol. Chem.* **279,** 23565–23573
24. Boron, W. F. (2006) *J. Am. Soc. Nephrol.* **17,** 2368–2382
25. Pappert, G., and Schubert, D. (1983) *Biochim. Biophys. Acta* **730,** 32–40
26. Casey, J. R., and Reithmeier, R. A. (1991) *J. Biol. Chem.* **266,** 15726–15737
27. Wang, D. N., Sarabia, V. E., Reithmeier, R. A., and Kuhlbrandt, W. (1994) *EMBO J.* **13,** 3230–3235
28. Pushkin, A. V., Tsuprun, V. L., Abuladze, N. K., Newman, D., and Kurtz, I. (2000) *IUBMB Life* **50,** 397–401
29. Pushkin, A., Sassani, P., Abuladze, N., Newman, D., Tatishchev, S., and Kurtz, I. (2001) *J. Am. Soc. Nephrol.* **12,** 8A
30. Gill, H. S., and Boron, W. F. (2006) *Acta Crystallogr. Sect. F Struct. Biol. Crystallogr. Commun.* **62,** 534–537
31. Ramjeesingh, M., Huan, L. J., Garami, E., and Bear, C. E. (1999) *Biochem. J.* **342,** 119–123
32. Bok, D., Schibler, M. J., Pushkin, A., Sassani, P., Abuladze, N., Naser, Z., and Kurtz, I. (2001) *Am. J. Physiol.* **281,** F920–F935
33. Casey, J. R., Lieberman, D. M., and Reithmeier, R. A. (1989) *Methods Enzymol.* **173,** 494–512
34. Rizzo, M. A., Springer, G. H., Granada, B., and Piston, D. W. (2004) *Nat. Biotechnol.* **22,** 445–449
35. van Rheenen, J., Langeslag, M., and Jalink, K. (2004) *Biophys. J.* **86,** 2517–2529
36. Azimov, R., Abuladze, N., Pushkin, A., Liu, W., Newman, D., and Kurtz, I. (2007) *FASEB J.* **21,** 1
37. Sassani, P., Pushkin, A., Gross, E., Gomer, A., Abuladze, N., Dukkipati, R., Carpenito, G., and Kurtz, I. (2002) *Am. J. Physiol.* **282,** C408–C416
38. Kurtz, I., Nagami, G., Yanagawa, N., Li, L., Emmons, C., and Lee, I. (1994) *J. Clin. Investig.* **94,** 173–183
39. Shepherd, F. H., and Holzenburg, A. (1995) *Anal. Biochem.* **224,** 21–27
40. Zheng, J., Du, G. G., Anderson, C. T., Keller, J. P., Orem, A., Dallos, P., and Cheatham, M. (2006) *J. Biol. Chem.* **281,** 19916–19924
41. Clarke, S. (1975) *J. Biol. Chem.* **250,** 5459–5469
42. Schubert, D. (1988) *Mol. Aspects Med.* **10,** 233–237
43. Rettig, M. P., Orendorff, C. J., Campanella, E., and Low, P. S. (2001) *Biochim. Biophys. Acta* **1515,** 72–81
44. Casey, J. R., Ding, Y., and Kopito, R. R. (1995) *J. Biol. Chem.* **270,** 8521–8527
45. Dolder, M., Walz, T., Hefti, A., and Engel, A. (1993) *J. Mol. Biol.* **231,** 119–132
46. Vince, J. W., Sarabia, V. E., and Reithmeier, R. A. (1997) *Biochim. Biophys. Acta* **1326,** 295–306
47. Sulistijo, E. S., and MacKenzie, K. R. (2006) *J. Mol. Biol.* **364,** 974–990
48. Mottamal, M., Zhang, J., and Lazaridis, T. (2006) *Proteins* **62,** 996–1009
49. Azimov, R., Abuladze, N., Pushkin, A., Liu, W., Newman, D., and Kurtz, I. (2007) *FASEB J.* **21,** A1283
50. Isacoff, E. Y., Jan, Y. N., and Jan, L. Y. (1990) *Nature* **345,** 530–534
51. Mathai, J. C., and Agre, P. (1999) *Biochemistry* **38,** 923–928
52. Emerick, M. C., and Fambrough, D. M. (1993) *J. Biol. Chem.* **268,** 23455–23459
53. Nicke, A., Rettinger, J., and Schmalzing, G. (2003) *Mol. Pharmacol.* **63,** 243–252
54. Sahin-Toth, M., Lawrence, M. C., and Kaback, H. R. (1994) *Proc. Natl. Acad. Sci. U. S. A.* **91,** 5421–5425
55. Kohler, K., Forster, I. C., Lambert, G., Biber, J., and Murer, H. (2000) *J. Biol. Chem.* **275,** 26113–26120
56. Bossi, E., Soragna, A., Miszner, A., Giovannardi, S., Frangione, V., and Peres, A. (2007) *Am. J. Physiol.* **292,** C1379–C1387
57. Wang, D. N., Kuhlbrandt, W., Sarabia, V. E., and Reithmeier, R. A. (1993) *EMBO J.* **12,** 2233–2239
58. Kedei, N., Szabo, T., Lile, J. D., Treanor, J. J., Olah, Z., Iadarola, M. J., and Blumberg, P. M. (2001) *J. Biol. Chem.* **276,** 28613–28619
59. Mitic, L. L., Unger, V. M., and Anderson, J. M. (2003) *Protein Sci.* **12,** 218–227
60. Xu, J., Liu, Y., Yang, Y., Bates, S., and Zhang, J. T. (2004) *J. Biol. Chem.* **279,** 19781–19789
61. AbdAlla, S., Lother, H., Langer, A., el Faramawy, Y., and Quitterer, U. (2004) *Cell* **119,** 343–354
62. Sahin-Toth, M., Frillingos, S., Bibi, E., Gonzalez, A., and Kaback, H. R. (1994) *Protein Sci.* **3,** 2302–2310
63. Chen, J. G., Liu-Chen, S., and Rudnick, G. (1997) *Biochemistry* **36,** 1479–1486
64. Sur, C., Schloss, P., and Betz, H. (1997) *Biochem. Biophys. Res. Commun.* **241,** 68–72
65. Lambert, G., Forster, I. C., Biber, J., and Murer, H. (2000) *J. Membr. Biol.* **176,** 133–141
66. Lambert, G., Forster, I. C., Stange, G., Kohler, K., Biber, J., and Murer, H. (2001) *J. Gen. Physiol.* **117,** 533–546
67. Kohler, K., Forster, I. C., Stange, G., Biber, J., and Murer, H. (2003) *Pfluegers Arch.* **446,** 203–210
68. Wittrup, K. D. (1995) *Curr. Opin. Biotechnol.* **6,** 203–208
69. Pajor, A. M., Krajewski, S. J., Sun, N., and Gangula, R. (1999) *Biochem. J.* **344,** 205–209
70. Tanaka, K., Zhou, F., Kuze, K., and You, G. (2004) *Biochem. J.* **380,** 283–287
71. Sitte, H. H., Farhan, H., and Javitch, J. A. (2004) *Mol. Interv.* **4,** 38–47
72. Gagnon, D. G., Bissonnette, P., and Lapointe, J. Y. (2006) *J. Gen. Physiol.* **127,** 145–158
73. Graveleau, C., Zaha, V. G., Mohajer, A., Banerjee, R. R., Dudley-Rucker, N., Steppan, C. M., Rajala, M. W., Scherer, P. E., Ahima, R. S., Lazar, M. A., and Abel, E. D. (2005) *J. Biol. Chem.* **280,** 31679–31685
74. Makagiansar, I. T., Nguyen, P. D., Ikesue, A., Kuczera, K., Dentler, W., Urbauer, J. L., Galeva, N., Alterman, M., and Siahaan, T. J. (2002) *J. Biol. Chem.* **277,** 16002–16010
75. Jha, B. K., Salunke, D. M., and Datta, K. (2002) *Eur. J. Biochem.* **269,** 298–306
76. Ellgaard, L., Molinari, M., and Helenius, A. (1999) *Science* **286,** 1882–1888
77. Kleizen, B., and Braakman, I. (2004) *Curr. Opin. Cell Biol.* **16,** 343–349
78. Chang, M.-H., Babcock, G. T., and Romero, M. F. (2007) *FASEB J.* **21,** A1282
79. Lindenthal, S., and Schubert, D. (1991) *Proc. Natl. Acad. Sci. U. S. A.* **88,** 6540–6544
80. Starremans, P. G., Kersten, F. F., Van Den Heuvel, L. P., Knoers, N. V., and Bindels, R. J. (2003) *J. Am. Soc. Nephrol.* **14,** 3039–3046
81. Ito, D., Koshino, I., Arashiki, N., Adachi, H., Tomihari, M., Tamahara, S., Kurogi, K., Amano, T., Ono, K., and Inaba, M. (2006) *J. Cell Sci.* **119,** 3602–3612
82. Ducoudret, O., Diakov, A., Muller-Berger, S., Romero, M. F., and Fromter, E. (2001) *Pfluegers Arch.* **442,** 709–717

Downloaded from www.jbc.org by guest, on September 29, 2009